

**Special Issue: Manufacturing of Advanced  
Biodegradable Polymeric Components**

**Guest Editors:** Prof. Roberto Pantani (University of Salerno) and  
Prof. Lih-Sheng Turng (University of Wisconsin-Madison)

**EDITORIAL**

**Manufacturing of advanced biodegradable polymeric components**

R. Pantani and L.-S. Turng, *J. Appl. Polym. Sci.* 2015, DOI: [10.1002/app.42889](https://doi.org/10.1002/app.42889)

**REVIEWS**

**Heat resistance of new biobased polymeric materials, focusing on starch, cellulose, PLA, and PHA**

N. Peelman, P. Ragaert, K. Ragaert, B. De Meulenaer, F. Devlieghere and Ludwig Cardon, *J. Appl. Polym. Sci.* 2015, DOI: [10.1002/app.42305](https://doi.org/10.1002/app.42305)

**Recent advances and migration issues in biodegradable polymers from renewable sources for food packaging**

P. Scarfato, L. Di Maio and L. Incarnato, *J. Appl. Polym. Sci.* 2015, DOI: [10.1002/app.42597](https://doi.org/10.1002/app.42597)

**3D bioprinting of photocrosslinkable hydrogel constructs**

R. F. Pereira and P. J. Bartolo, *J. Appl. Polym. Sci.* 2015, DOI: [10.1002/app.42458](https://doi.org/10.1002/app.42458)

**ARTICLES**

**Largely toughening biodegradable poly(lactic acid)/thermoplastic polyurethane blends by adding MDI**

F. Zhao, H.-X. Huang and S.-D. Zhang, *J. Appl. Polym. Sci.* 2015, DOI: [10.1002/app.42511](https://doi.org/10.1002/app.42511)

**Solubility factors as screening tools of biodegradable toughening agents of polylactide**

A. Ruellan, A. Guinault, C. Sollogoub, V. Ducruet and S. Domenek, *J. Appl. Polym. Sci.* 2015, DOI: [10.1002/app.42476](https://doi.org/10.1002/app.42476)

**Current progress in the production of PLA-ZnO nanocomposites: Beneficial effects of chain extender addition on key properties**

M. Murariu, Y. Paint, O. Murariu, J.-M. Raquez, L. Bonnaud and P. Dubois, *J. Appl. Polym. Sci.* 2015, DOI: [10.1002/app.42480](https://doi.org/10.1002/app.42480)

**Oriented polyvinyl alcohol films using short cellulose nanofibrils as a reinforcement**

J. Peng, T. Ellingham, R. Sabo, C. M. Clemons and L.-S. Turng, *J. Appl. Polym. Sci.* 2015, DOI: [10.1002/app.42283](https://doi.org/10.1002/app.42283)

**Biorenewable polymer composites from tall oil-based polyamide and lignin-cellulose fiber**

K. Liu, S. A. Madbouly, J. A. Schrader, M. R. Kessler, D. Grewell and W. R. Graves, *J. Appl. Polym. Sci.* 2015, DOI: [10.1002/app.42592](https://doi.org/10.1002/app.42592)

**Dual effect of chemical modification and polymer precoating of flax fibers on the properties of the short flax fiber/poly(lactic acid) composites**

M. Kodal, Z. D. Topuk and G. Ozkoc, *J. Appl. Polym. Sci.* 2015, DOI: [10.1002/app.42564](https://doi.org/10.1002/app.42564)

**Effect of processing techniques on the 3D microstructure of poly(L-lactic acid) scaffolds reinforced with wool keratin from different sources**

D. Puglia, R. Ceccolini, E. Fortunati, I. Armentano, F. Morena, S. Martino, A. Aluigi, L. Torre and J. M. Kenny, *J. Appl. Polym. Sci.* 2015, DOI: [10.1002/app.42890](https://doi.org/10.1002/app.42890)

**Batch foaming poly(vinyl alcohol)/microfibrillated cellulose composites with CO<sub>2</sub> and water as co-blowing agents**

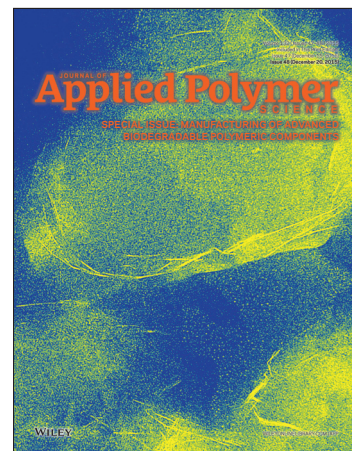
N. Zhao, C. Zhu, L. H. Mark, C. B. Park and Q. Li, *J. Appl. Polym. Sci.* 2015, DOI: [10.1002/app.42551](https://doi.org/10.1002/app.42551)

**Foaming behavior of biobased blends based on thermoplastic gelatin and poly(butylene succinate)**

M. Oliviero, L. Sorrentino, L. Caferio, B. Galzerano, A. Sorrentino and S. Iannace, *J. Appl. Polym. Sci.* 2015, DOI: [10.1002/app.42704](https://doi.org/10.1002/app.42704)

**Reactive extrusion effects on rheological and mechanical properties of poly(lactic acid)/poly[(butylene succinate)-co-adipate]/epoxy chain extender blends and clay nanocomposites**

A. Mirzadeh, H. Ghasemi, F. Mahrous and M. R. Kamal, *J. Appl. Polym. Sci.* 2015, DOI: [10.1002/app.42664](https://doi.org/10.1002/app.42664)



**Special Issue: Manufacturing of Advanced  
Biodegradable Polymeric Components**

**Guest Editors:** Prof. Roberto Pantani (University of Salerno) and  
Prof. Lih-Sheng Turng (University of Wisconsin-Madison)

**Rotational molding of biodegradable composites obtained with PLA reinforced by the wooden backbone of opuntia ficus indica cladodes**

A. Greco and A. Maffezzoli, *J. Appl. Polym. Sci.* 2015, DOI: [10.1002/app.42447](https://doi.org/10.1002/app.42447)

**Foam injection molding of poly(lactic) acid: Effect of back pressure on morphology and mechanical properties**

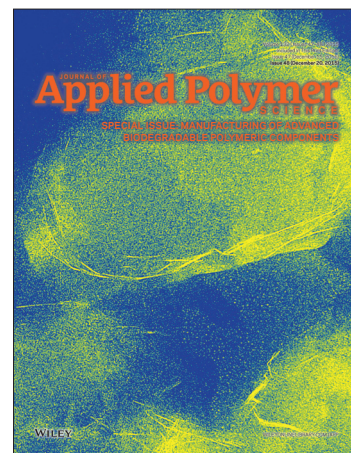
V. Volpe and R. Pantani, *J. Appl. Polym. Sci.* 2015, DOI: [10.1002/app.42612](https://doi.org/10.1002/app.42612)

**Modification and extrusion coating of polylactic acid films**

H.-Y. Cheng, Y.-J. Yang, S.-C. Li, J.-Y. Hong and G.-W. Jang, *J. Appl. Polym. Sci.* 2015, DOI: [10.1002/app.42472](https://doi.org/10.1002/app.42472)

**Processing and properties of biodegradable compounds based on aliphatic polyesters**

M. R. Nobile, P. Cerruti, M. Malinconico and R. Pantani, *J. Appl. Polym. Sci.* 2015, DOI: [10.1002/app.42481](https://doi.org/10.1002/app.42481)



## Processing and properties of biodegradable compounds based on aliphatic polyesters

Maria Rossella Nobile,<sup>1</sup> Pierfrancesco Cerruti,<sup>2</sup> Mario Malinconico,<sup>2</sup> Roberto Pantani<sup>1</sup>

<sup>1</sup>Department of Industrial Engineering, University of Salerno, Fisciano (SALERNO), Italy

<sup>2</sup>IPCB - Consiglio Nazionale delle Ricerche - Pozzuoli Na - Italy

Correspondence to: M. R. Nobile (E-mail: mrnobile@unisa.it)

**ABSTRACT:** Two aliphatic biodegradable polyesters, Poly(butylene succinate) and Poly(lactic acid), are selected together with two inorganic fillers, talc and TiO<sub>2</sub>, to obtain biodegradable compounds for replacing polystyrene in the production of disposable plastic cups and plates. The rheological behavior of the pure polymers and the compounds is investigated, the mechanical properties of the compounds are determined in terms of modulus and elongation at break, the heat distortion temperature of the compounds is measured and compared to those of pure PBS and PS. Finally, the biodegradation of the compounds is also investigated. The processability and the final properties, in terms of elastic modulus and heat distortion temperature, make these compounds interesting for the production of disposable plates and cups for hot food and beverages, also considering that the elongation at break is significant. Furthermore, the results of biodegradation tests in composting conditions show that the presence of TiO<sub>2</sub> induces a lag time and lower values of biodegradation. © 2015 Wiley Periodicals, Inc. *J. Appl. Polym. Sci.* **2015**, *132*, 42481.

**KEYWORDS:** biopolymers and renewable polymers; manufacturing; mechanical properties; polyesters; rheological properties

Received 2 March 2015; accepted 6 May 2015

DOI: 10.1002/app.42481

### INTRODUCTION

The use of biodegradable or bio-based polymers for replacing their durable counterparts has become highly attracting for industries involved in the production of disposable plates and cups. It is indeed quite obvious that the environmental impact of this class of products will be dramatically reduced if a suitable biodegradable material would be selected. The required properties for a good substitute of polystyrene (the most commonly adopted polymer for these applications) are: a good processability in terms of viscosity; a high elastic modulus, coupled with a low fragility; a high heat distortion temperature (HDT); the lowest possible cost. This combination of properties is beyond the possibilities of the most common commercial polymers.

Poly(butylene succinate) (PBS),<sup>1–3</sup> for instance, presents a high flexibility, excellent impact strength, a good melt processability, and a high thermal resistance. However, mechanical properties like tensile modulus and strength are definitely too poor. Adding a suitable filler, which can also have the advantage of decreasing the cost of the compound, can attain some improvements. For instance, it is quite well known that talc, due to its platy nature, can effectively increase stiffness, heat distortion temperature, creep resistance, tensile and flexural strength.

Besides the use of additives, other methods like blending polymers with different properties, can produce the desired material which could satisfy specific requirements.<sup>4–8</sup> At this regard, among biodegradable polymers,<sup>9–17</sup> Poly(lactic acid) (PLA)<sup>9–11</sup> is a biodegradable polyester which presents a much higher elastic modulus and strength than PBS but its inherent brittleness significantly impedes its wide applications in many fields and, in particular, makes it inadequate for the chosen application. Furthermore, the poor resistance of PLA to high temperature does not allow its use for the contact with hot food or beverages. Blending PBS and PLA can, then, represent the appropriate method to obtain a biodegradable material that keeps the excellent properties of PBS while increasing its tensile modulus and strength.

Blends of PLA and PBS were, indeed, studied in the literature in order to obtain a material with intermediate properties.<sup>18–24</sup> It was reported that the PLA/PBS polymer blends are partially miscible in the amorphous region<sup>18,20</sup> and substantially immiscible in the crystalline phase<sup>19,21</sup> and that PLA dispersed phases in blends with PBS percentages above 50% act as an effective reinforcement<sup>24</sup> due to their ellipsoidal shape with high aspect ratio (length/diameter). Recently, composites and nano composites,<sup>25–29</sup> based on biodegradable polymers, were also investigated in the literature.

**Table I.** Typical Properties of the Polymers Adopted in this Study

	PBS	PLA	PS
Melt flow rate (190°C) (g/10 min)	25	10–80	3
Tensile Modulus (MPa)	500	3700	2500
Tensile yield strength (MPa)	35	50	50
Tensile elongation at break	300%	2.5%	5%
Heat Distortion Temperature (°C)	94	60	94

The purpose of this study is to find biodegradable polymeric compounds that can replace the use of polystyrene for the production of disposable plates and cups for hot food or beverages. At this regard, two aliphatic biodegradable polyesters, PBS and PLA, were selected together with two inorganic fillers: talc, which has a low cost and is effective in increasing the modulus and the HDT of polymers, and TiO<sub>2</sub>, which is a commonly adopted white pigment for the industry of plastic cups and plates. The rheological behavior of the pure polymers and the compounds was investigated, the mechanical properties of the compounds were determined in terms of modulus and elongation at break, the heat distortion temperature of the compounds was measured and compared to that of pure PBS and PS. Finally, the biodegradation of the compounds was also investigated.

## EXPERIMENTAL

### Materials

The Poly(butylene succinate), PBS, adopted in this study was supplied by Fuwin New Material Co., Ltd (China) with the commercial name of ECONORM 1201. The main characteristics of PBS, of interest for this study, are reported in Table I. Two PLA grades produced by Natureworks were adopted: an extrusion grade, 4032D, and an injection molding grade, 3251D. These two grades will be referred to as “extrusion” and “injection” grade PLA in the following. Also for PLA, the typical values of relevant properties are reported in Table I. The differences in mechanical properties between the PLA and PBS resins are evident from the table: PBS presents a much lower tensile modulus and strength than PLA while it is characterized by a much higher elongation at break and heat distortion temperature.

A general-purpose talc, PREVER M10 IMERYS, with a median diameter of about 3 micron was chosen for this study. Rutile titanium dioxide pigment (TiO<sub>2</sub>) supplied by Dow Chemicals with the name Ti-Pure R-103 was used as a whitening agent. For comparison, also a polystyrene (PS 158K supplied by BASF) commonly adopted for the production of disposable cups and plates was characterized.

### Sample Preparation

The compounds were produced by starve-feeding the components directly into the hopper of a single screw extruder, model TEACH-LINE E20T (COLLIN), L/D 25. The temperature profile along the extruder was chosen to limit the thermal degradation of the materials.<sup>30</sup> In particular, an increasing temperature from 150°C (in the feed section) to 190°C (in the metering section),

was set. The screw speed was set at 38 rpm. The neat PBS and PLA extrusion and injection grade polymers were also extruded. The extruder was equipped with a flat die and chill rolls at a temperature of 12.5°C. The obtained films had a thickness of 0.30 ± 0.04 mm.

Three compounds were produced and coded with letters A, B and C, as summarized in Table II. Finally, the corresponding compounds without the TiO<sub>2</sub> whitening agent were also prepared, named A\*, B\* and C\*, whose compositions are reported in Table II. Before testing the neat PBS and PLA polymers as well as the compounds were dried under vacuum at  $T = 60^\circ\text{C}$  for 24 h.

### Methods

Thermal analysis was conducted by a Differential Scanning Calorimetry (DSC) Mettler Toledo DSC 820 apparatus. Tests were carried out on the neat PBS and PLA polymers and on the compounds. Samples of the films of about 10 mg were heated up under dry nitrogen purge gas from 20°C to 200°C at a heating rate of 10°C/min and then cooled down from 200°C to 20°C at a cooling rate of 10°C/min.

Rheological measurements in the molten state have been performed on the pure PBS and PLA samples, as well as on the compounds summarized in Table II to investigate their processability. The rheological behavior of polystyrene was also analyzed.

The frequency dependence of the oscillatory shear complex viscosity was evaluated by a strain-controlled ARES (TA) rotational rheometer equipped with a parallel plate geometry (25 mm diameter, 1 mm gap). Strain sweep tests, at the frequency of 10 rad/s and  $T = 190^\circ\text{C}$ , were previously performed to determine the linear viscoelastic region. Small amplitude oscillatory shear measurements, within the linear viscoelasticity regime, were then performed in the frequency range comprised between 10<sup>-2</sup> and 10<sup>2</sup> rad/s, at the temperatures of 180, 190, and 200°C.

The transient shear stress ( $\sigma$ ) response at  $T = 190^\circ\text{C}$  for the two PBS/PLA/Talc 55/25/20 compounds, B\* and C\*, at different shear rates has been investigated in start-up shear flow experiments using a strain-controlled ARES (TA) rotational rheometer in cone-plate configuration (cone angle 0.1 rad, plate diameter 25 mm) in order to evaluate the steady-state viscosity values of the compounds and to assess their stability at high temperatures.

**Table II.** Composition of the Compounds

	A	A*	B	B*	C	C*
PBS	67%	70%	50%	55%	50%	55%
PLA extrusion grade			25%	25%		
PLA injection grade					25%	25%
Talc	27%	30%	20%	20%	20%	20%
TiO <sub>2</sub>	6%		5%		5%	

Both the rotational dynamic and steady shear viscosity measurements were performed under a continuous nitrogen purge. Capillary rheological measurements were aimed at verifying the processability of the materials. Therefore, the range of shear rates investigated was that of interest for processing, namely above about 10/s. Capillary rheological measurements were carried out by a RH7 Flowmaster Bohlin rheometer. The measurements were carried out at the temperature of 190°C. The capillary used had a diameter of 1 mm and a length of 30 mm. The data were corrected for entry effects. The Rabinowitsch correction was also applied to the raw data and the steady shear viscosity in the high shear rate range was evaluated.

Tensile tests were performed using a dynamometer INSTRON 5564 equipped with a load cell of 1.0 KN. The measurements were conducted at a constant deformation rate of 10 mm/min. For each studied sample 5 specimens (dog-bone shaped), with the following standard sizes: Width = 4.2 mm; Length = 28 mm; Thickness = 0.3 mm, were analyzed. Before performing the measurements, the samples were conditioned in a climate chamber with a moisture content of 50% relative and  $T = 25^\circ\text{C}$ .

The engineering stress,  $\sigma_E$ , was calculated as the ratio between the force measured by the instrument and the initial section of the specimen (width · thickness). The engineering strain,  $\varepsilon_E$ , was calculated as the ratio between the increase of length and the initial length of the specimen. Due to the high elongations reached, it was chosen to calculate also the true strain,  $\varepsilon_T$  and stress,  $\sigma_T$ . In particular, the following equations were adopted:

$$\begin{aligned}\sigma_T &= \ln(\varepsilon_E + 1) \\ \sigma_T &= \sigma_E(\varepsilon_E + 1)\end{aligned}\quad (1)$$

The heat distortion temperature, HDT, was determined following the procedure outlined in ASTM D648 standard. The test samples were subjected to a bending load on three points. The stress used for the test was 0.45 MPa, and the temperature was increased at a rate of 120°C/h, until the samples reached a deformation of 0.25 mm.

Biodegradation tests were carried out in a homemade respirometric system, as assessed by ASTM D 5338 and ISO 14855 standards.<sup>31</sup> A schematic representation of the system is shown in Figure 1.

Yard waste compost was obtained from a municipal composting plant located in Salerno. The compost was screened through a 1 cm sieve to separate large inert objects from the compost. To determine the total dry solids, the compost was dried in an oven at 105°C for 6 h and weighed before and after drying. The amount of volatile solids, i.e. the amount of organic matter present in the compost, was obtained by subtracting the residue after incineration at about 550°C from the total dry solids of the same sample. Cellulose was used as a positive control.

Each reactor was loaded with 100 g of specimen, 50 g of Vermiculite, and 600 g of compost. The CO<sub>2</sub> produced by the compost alone was controlled by preparing a reactor without polymer. During the entire duration of the test, moisture, mixing and aeration of all the reactors were periodically controlled as established by the norms.

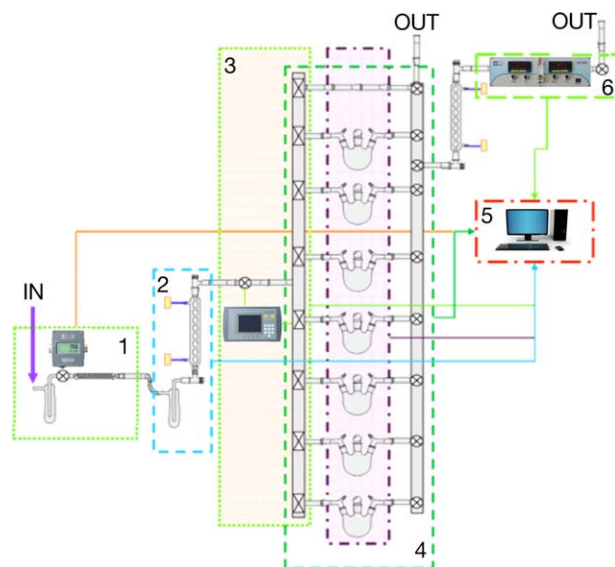


**Figure 1.** Schematic representation of the respirometric apparatus. (1) air pumping system; (2) CO<sub>2</sub> trap and dryers; (3) control of air supply at a constant flow rate of 0.5 L/min to each bioreactor; (4) bioreactors, having approximately three litres internal volume kept at constant temperature of  $58 \pm 2^\circ\text{C}$ ; (5) data acquisition system and control; (6) infrared analyzer. [Color figure can be viewed in the online issue, which is available at wileyonlinelibrary.com.]

The test was considered valid only if the reactor filled with compost produced an amount of CO<sub>2</sub> ranging between 50 and 150 mg per gram of volatile solid in the first 10 days of incubation.

The molar concentration of CO<sub>2</sub> determined by the infrared analyzer was elaborated according to the following equation:

$$g\text{CO}_2 = F \cdot t \cdot c \cdot P_{\text{mco}_2} \quad (2)$$

where  $g\text{CO}_2$  is the mass of CO<sub>2</sub> coming out from each reactor;  $F$  is the gas Flow rate (mol/min);  $P_{\text{mco}_2}$  is the molecular weight of CO<sub>2</sub> (44 g/mol). The mineralization (Min) is then estimated by the following equation:

$$\text{Min} = \frac{g\text{CO}_2 - g\text{CO}_2b}{g\text{CO}_2\text{mat}} \quad (3)$$

where  $g\text{CO}_2b$  is the amount of CO<sub>2</sub> produced by the compost and  $g\text{CO}_2\text{mat}$  is the theoretical amount of CO<sub>2</sub> that can be released by the sample upon total oxidation of incubated materials. In the latter term the amount of inorganic filler (Talc and TiO<sub>2</sub>) was obviously not considered.

## RESULTS AND DISCUSSION

### Thermal Properties

The results of calorimetric tests are reported in Figure 2 for the compounds A, B, and C. In particular, the first heating scan is reported in Figure 2(a). It can be noticed that the compound A presents only the melting peak of the PBS at about 117°C. The compounds B and C present a glass transition temperature,  $T_g$ , at about 60°C (which can be ascribed to the PLA fraction), a melting peak at about 117°C (similar to the one found for compound A and due to the PBS fraction) and another, smaller

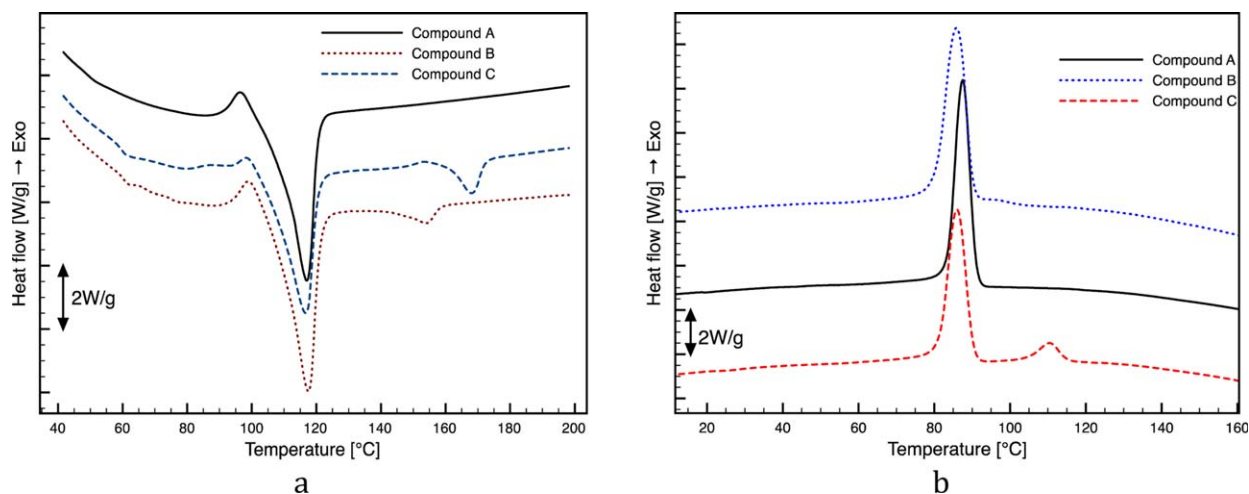


**Figure 2.** DSC results for compounds. (a) First heating and (b) cooling. [Color figure can be viewed in the online issue, which is available at [wileyonlinelibrary.com](http://wileyonlinelibrary.com).]

melting peak at 153°C (for compound B, containing the extrusion grade PLA) and 168°C (for compound C, containing the injection molding grade PLA) due to the PLA fraction. The  $T_g$  of the PBS fraction is not detected since it is at about  $-33^\circ\text{C}$ , out of the temperature window here investigated. The presence of separated features due to each of the polymers in the compound B confirms the immiscibility of the two resins. Similar results are also found in the analysis of the cooling scan, reported in Figure 2(b). The compound A presents a clear crystallization peak at 88°C, due to PBS. The compound C, containing the injection molding grade PLA also presents a crystallization peak of PLA at 111°C. In this case, the crystallization peak due to PBS moves toward lower temperatures (about 2°C lower). This could indicate an inhibition effect of PLA on the crystallization of PBS. The compound B, containing the extrusion grade PLA, does not show any crystallization peak due to PLA, but just a small shoulder soon before PBS crystallization peak at about 95°C.

### Rheological Properties

The complex viscosity ( $\eta^*$ ) for the PS, the PBS, and the two PLA pure polymers was measured as a function of temperature ( $T$ ) and frequency ( $\omega$ ). The  $\eta^*$  values obtained at various temperatures for the samples were shifted along the frequency axis to obtain the master curves shown in Figure 3(a,b) at the reference temperature ( $T_0$ ) of 190°C. The time-temperature superposition principle (TTS)<sup>32</sup> was applicable over the entire temperature range. The temperature dependence of the shift factors can be expressed in terms of an Arrhenius relationship [eq. (4)]:

$$a_T = \exp \left[ \frac{E_a}{R} \left( \frac{1}{T} - \frac{1}{T_0} \right) \right] \quad (4)$$

where  $R$  is the universal gas constant,  $E_a$  is activation energy for flow and  $T_0$  is the reference temperature. The calculated  $E_a$  for flow at the reference temperature of 190°C for the pure polymers are reported in Table III.

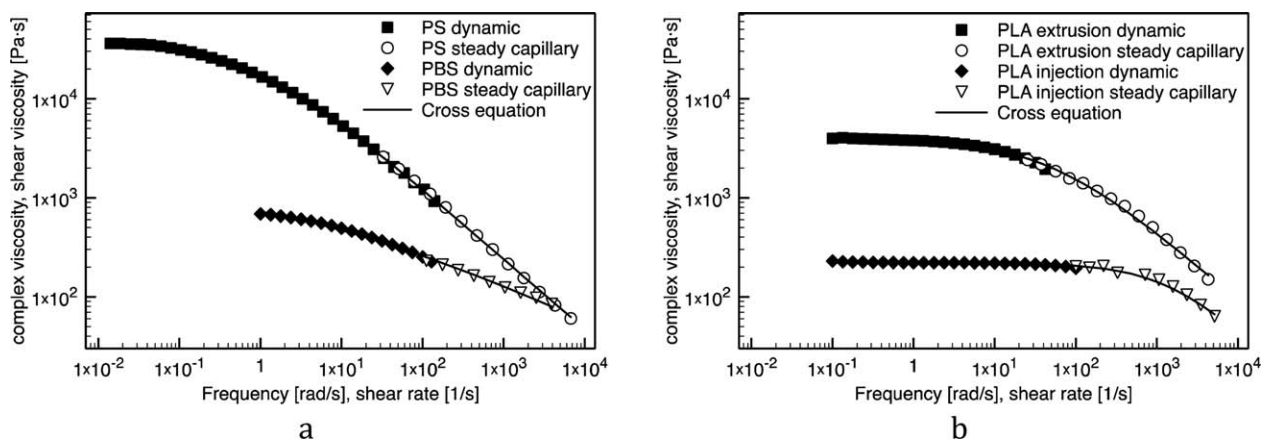


**Figure 3.** Complex viscosity and capillary steady shear viscosity of: (a) pure PS and PBS; (b) pure PLA extrusion and injection molding grade.  $T_0 = 190^\circ\text{C}$ . Filled symbols represent dynamic data. Empty symbols represent steady capillary data. The continuous lines correspond to the Cross Model model [eq. (6)] fit to the viscosity data.

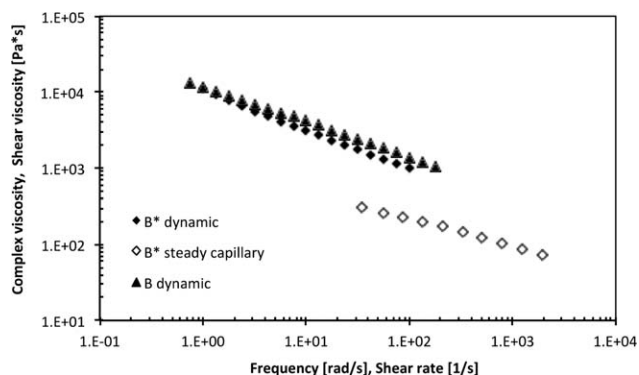
**Table III.** Fitting Parameters of the Cross Model and Activation Energy for the Pure Polymers

	PS	PBS	PLA extrusion grade	PLA injection grade
$\eta_0$ [Pa s]	38054	1213	4016	221
$\tau$ [s]	1.25	0.34	0.020	0.0005
$n$	0.29	0.63	0.29	0.125
$E_a$ [kcal/mol]	25.5	11.1	15.5	24.5

The PS, the PBS and the PLA extrusion grade polymers show shear thinning behavior at higher frequencies and a Newtonian behavior at the lower frequencies while the PLA injection molding grade polymer is characterized by a Newtonian behavior in the whole frequency range tested, as evident in Figure 3(a,b).

In Figure 4 the complex viscosity versus frequency for both the PBS/PLA/Talc/TiO<sub>2</sub> 55/20/20/5 (compound B) and the PBS/PLA/Talc 55/25/20% w/w (compound B\*) is reported. The strain amplitude used was as low as 0.4% because the linear viscoelastic limit of only  $\sim 0.5\%$  was detected for these samples. The complex viscosity results evidence a strong shear thinning trend also at the lower frequencies investigated. The  $\eta^*$  values for the B and B\* compounds run very close indicating that the small difference in composition has no relevant effect on the dynamic shear behavior of the two systems. In the following, therefore, the rheological results are shown only for the compounds without the whitening TiO<sub>2</sub>, namely the compounds B\* and C\*.

The steady shear viscosity values of the pure materials obtained by capillary measurements are also reported in Figure 3(a,b). The Cox-Merz<sup>33</sup> rule states that the steady shear viscosity is numerically equal to the complex viscosity obtained from small-amplitude measurements on polymer melts and polymeric solutions. In our case the capillary viscosity data very well correlate with the oscillatory shear viscosities indicating that the Cox-Merz law holds for the pure polymers. On the other hand the

**Figure 4.** Viscosity measurements carried out on Compounds B and B\*.  $T = 190^\circ\text{C}$ .

rule clearly fails in the case of the compounds for which the capillary steady state viscosity measurements do not correlate with the complex viscosity values, being one order of magnitude lower than the corresponding complex viscosity, as presented in Figure 4 for the compound B\*.

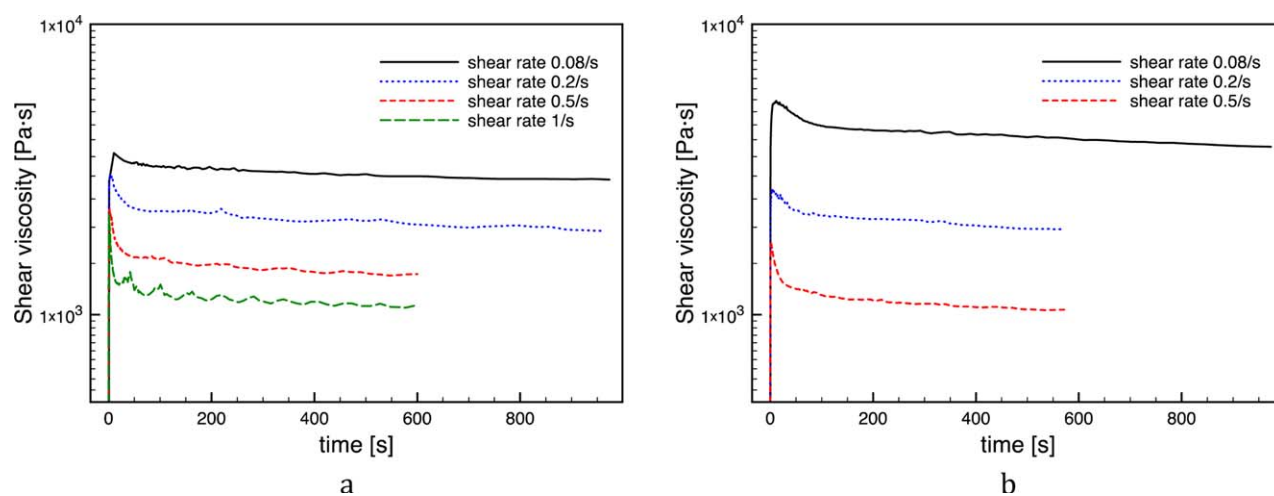
The zero shear viscosity  $\eta_0$  at  $T = 190^\circ\text{C}$  of the investigated pure samples was evaluated from the master curves as the limiting value of the complex viscosity:

$$\eta_0 = \lim_{\omega \rightarrow 0} \eta^* \quad (5)$$

In the case of PS and PLA samples, there is a clear plateau in the viscosity at the lowest frequencies, indicating that the Newtonian region has been reached in the frequency window investigated. In contrast, the limiting region was not clearly observed for the pure PBS. In all the cases, the estimate of  $\eta_0$  was obtained using a fit of all the experimental viscosity data to the Cross model [eq. (6)], as shown in Figure 3(a,b)

$$\eta = \frac{\eta_0}{1 + (\tau \dot{\gamma})^{1-n}} \quad (6)$$

where  $\eta_0$ ,  $\tau$  and  $n$  are the fitting parameters and  $\dot{\gamma}$  is the shear rate. The corresponding values for the pure polymers are reported in Table III.

**Figure 5.** Transient shear viscosity for the compounds: (a) B\* and (b) C\*.  $T = 190^\circ\text{C}$ . [Color figure can be viewed in the online issue, which is available at [wileyonlinelibrary.com](http://wileyonlinelibrary.com).]

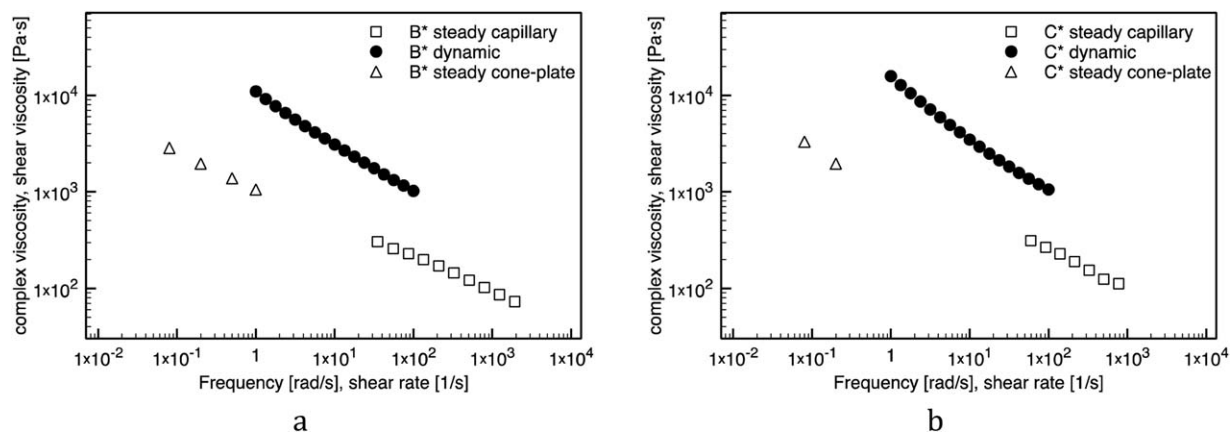


Figure 6. Complex viscosity, cone-plate and capillary steady shear viscosity of compounds: (a) B\* and (b) C\*.  $T = 190^{\circ}\text{C}$ .

To evaluate the steady shear viscosity at low shear rates for the compounds B\* and C\* it was necessary to perform transient shear experiments. The transient shear viscosity response at  $T = 190^{\circ}\text{C}$  obtained in start-up shear flow experiments for the compounds B\* and C\* at different shear rates is reported in Figure 5(a,b). It is shown that at the lower shear rates the viscosity gradually approached the steady state, while increasing the shear rates an overshoot appeared before the viscosity approached the steady value. This overshoot is a typical non-linear response of the polymer related to the entanglement resistance to the flow. The steady shear viscosity values were evaluated for the compounds B\* and C\* at the different shear rates and, then, used to obtain the flow curves of the compounds presented in Figure 6(a,b).

Moreover, the transient experiments also allowed to ascertain the thermal stability of the compounds at high temperatures for times longer than 600 s. For processing the residence times at high temperature inside the machines is of the order of 10 min. Then, the investigated compounds can be considered suitable for processing operations.

The steady shear viscosity from cone-plate and capillary measurements are presented in Figure 6(a,b) for the B\* and C\* compounds, respectively. A good correlation between the cone and plate and capillary data is observed. In the same Figure the oscillatory shear viscosity data are also reported. For both the compounds the steady-state viscosity is one order of magnitude lower than the corresponding complex viscosity, showing that the imposed shear flow significantly modifies the compound structure with the dispersed PLA phase orienting along the shear direction. Again, as discussed above, it is clearly evidenced that the Cox-Merz law fails in the case of compounds, analogously to what reported for the case of carbon nanotube polymer composites,<sup>34</sup> carbon nanofiber composites,<sup>35</sup> as well as polymer-layered silicate composite,<sup>36</sup> above the percolation threshold.

Finally, the steady-state shear viscosity flow curve of the B\* and C\* compounds is compared with flow curve of polystyrene in Figure 7. Both the compounds present a lower viscosity than PS at high shear rates, indicating a better processability in the range of interest for extrusion and injection molding. At low

shear rates, the viscosity of the compounds, even if still lower than that of PS, reaches considerable values, making these materials suitable for processes like thermoforming, in which a high viscosity is needed at low shear rates to reduce the free flow of the material.

#### Mechanical Properties

The mechanical tests carried out on the specimens of compounds A and C are reported in Figures 8 and 9, respectively. It can be immediately noticed that, in spite of the large amount of filler, the compound A presents a considerable elongation at break, due to the PBS phase. The measurements present a good reproducibility, and the results of mechanical tests are summarized in Table IV together with those for the compound B.

It can be noticed that the inorganic fillers cause an increase of the modulus of a factor of more than 2 in Compound A with respect to pure PBS. However, considering that the elastic modulus of PS, which is the reference material for the target application, is about 2500 MPa, the modulus of Compound A is still too low. The Compounds B and C present a larger modulus, intermediate between those of pure PLA and PBS. The reached value makes these compounds interesting for the production of disposable plates and cups. The elongation at break is also

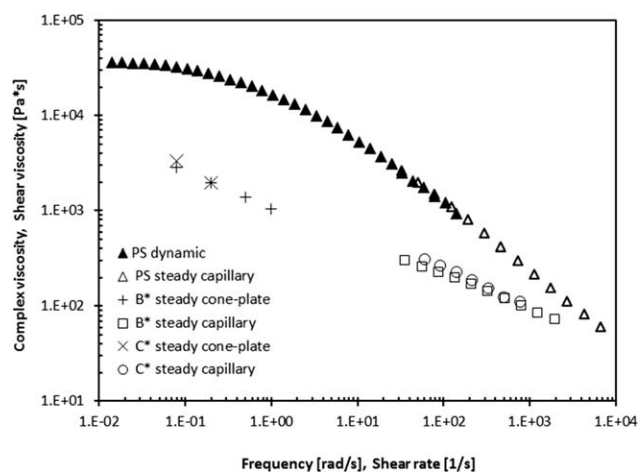
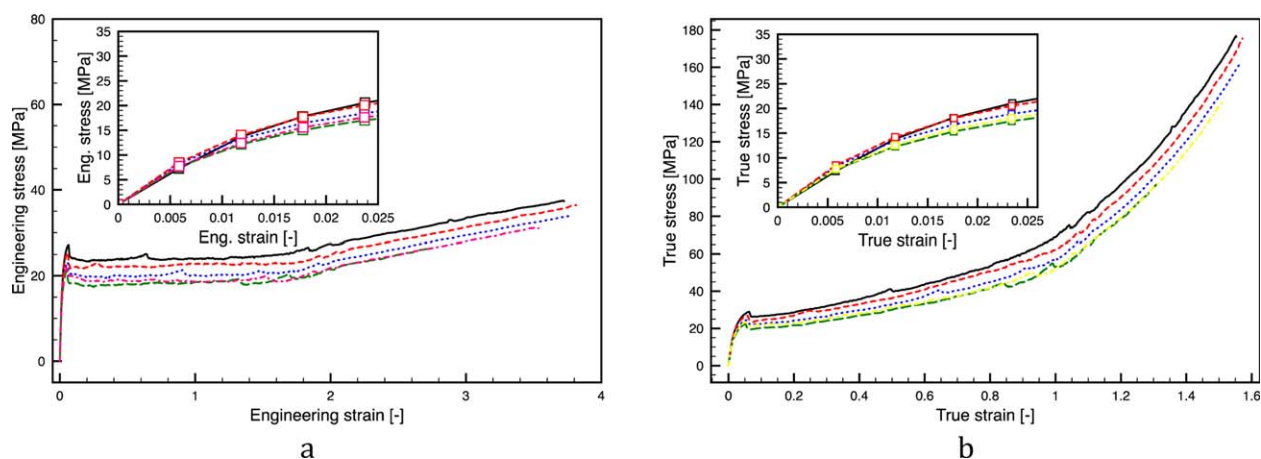
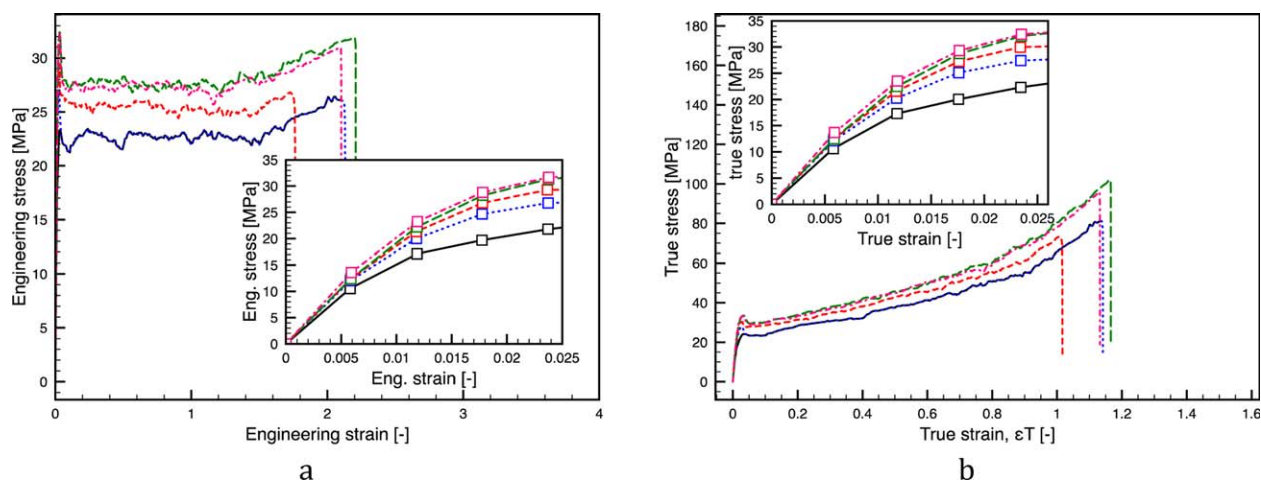


Figure 7. Flow curves for Polystyrene, compounds B\* and C\*.  $T = 190^{\circ}\text{C}$ .





**Figure 8.** Mechanical tests carried out on specimens of Compound A. (a) Engineering curves; (b) True curves. [Color figure can be viewed in the online issue, which is available at [wileyonlinelibrary.com](http://wileyonlinelibrary.com).]



**Figure 9.** Mechanical tests carried out on specimens of Compound C. (a) Engineering curves; (b) True curves. [Color figure can be viewed in the online issue, which is available at [wileyonlinelibrary.com](http://wileyonlinelibrary.com).]

considerable. Similar mechanical results were also obtained for the B\* and C\* compounds.

#### Heat Distortion Temperature

The HDTs measured on the compounds is reported in Table V. This is one of the most interesting results reached in this study. The Compound A presents a higher HDT than the pure PBS (which is about 94°C) due to the addition of inorganic fillers. The Compounds B\* and C\* present a HDT similar to that of

pure PBS, and much higher with respect to pure PLA whose HDT is 60°C, as reported in the literature. Both B\* and C\* compounds are, then, characterized by HDTs high enough to be used as plates and cups for hot food or beverages.

#### Biodegradation

The results of biodegradation tests in composting conditions are reported in Figure 10. It can be noticed that Compounds A and C, that include the TiO<sub>2</sub> whitening agent, present a lag time of

**Table IV.** Summary of Results of Mechanical Tests

	Compound A	Compound B	Compound C
Elastic Modulus (E) [MPa]	1326 ± 70	1960 ± 40	1993 ± 210
Yield stress [MPa]	23.6 ± 2	26.3 ± 1	28.6 ± 3
Stress at break [GPa] engineering	33.4 ± 2	26.8 ± 2	27.9 ± 3
Stress at break [GPa] true	160 ± 11	87 ± 10	87 ± 11
Deformation at break [%] engineering	365 ± 10	186 ± 18	190 ± 20
Deformation at break [%] true	156 ± 1	110 ± 5	114 ± 4

**Table V.** Heat Distortion Temperatures

Materials	HDT [°C] (120°C/h –0.45 MPa)
PBS	94
Compound A	98
Compound B*	96
Compound C*	94
PS	82

about 5 days before biodegradation starts. Afterwards, biodegradation proceeds to reach a value of about 20% for Compound A and 30% for Compound C. The faster biodegradation of Compound C (that includes also PLA) with respect to Compound A was expected, on the basis of the slower biodegradation rate of PBS with respect to PLA.<sup>31,37</sup> The lag time, and the relatively slow biodegradation rate, could be ascribed to the presence of TiO<sub>2</sub>. Indeed, it is known from literature<sup>38</sup> that the enzymatic hydrolysis of PLA can be inhibited by rutile-type TiO<sub>2</sub> particles. The compound B, not reported, showed a behavior very similar to the compound C.

In order to elucidate the effect of TiO<sub>2</sub>, compounds A\* and C\* were also subjected to biodegradation tests (Figure 10). It can be noticed that the lag time disappears: the biodegradation starts immediately. Furthermore, the amount of mineralization after 50 days is much larger with respect to the corresponding compounds with TiO<sub>2</sub>. The biodegradation rate of Compound C\* is larger than that of Compound A\*, reaching a mineralization of about 40% in 50 days.

A visual observation of the samples is reported in Figure 11, in which micrographs of the section of films which underwent biodegradation in compost for 40 days are reported. The difference in color between compounds with (micrographs on the left) and without TiO<sub>2</sub> (micrographs on the right) is evident. The samples without TiO<sub>2</sub> are darker for the lack of the whitening pigment. It can be also noticed that all the Compounds present a rather homogeneous structure, whereas Compound

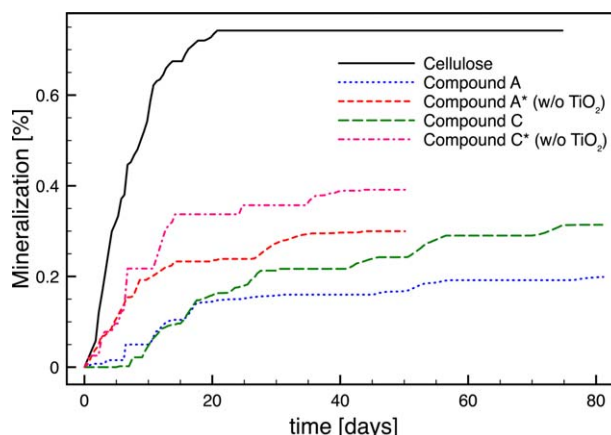


**Figure 10.** Results of biodegradation tests in compost at 58°C. [Color figure can be viewed in the online issue, which is available at wileyonlinelibrary.com.]

C\* presents a more degraded surface layer. This suggests the presence of a considerable surface erosion mechanism, which is not so relevant in the other compounds. In particular, by comparison with the Compound C, it can be concluded that this mechanism is inhibited by the presence of TiO<sub>2</sub>.

This effect of TiO<sub>2</sub> is interesting, considering that this filler can be adopted for modulating the biodegradation rate of the Compounds.

## CONCLUSIONS

In this study biodegradable polymeric compounds were processed and analyzed with the aim of finding biodegradable substitutes for polystyrene for the production of disposable plates and cups for hot food and beverages. In particular, two biodegradable polymers were selected: PBS, which presents a high flexibility, an excellent impact strength, a good melt processability, good thermal resistance, but low tensile modulus and strength; and PLA, which has a much higher modulus, but a very low deformation at break and an inadequate HDT. Furthermore, two inorganic fillers were selected: talc, which has a

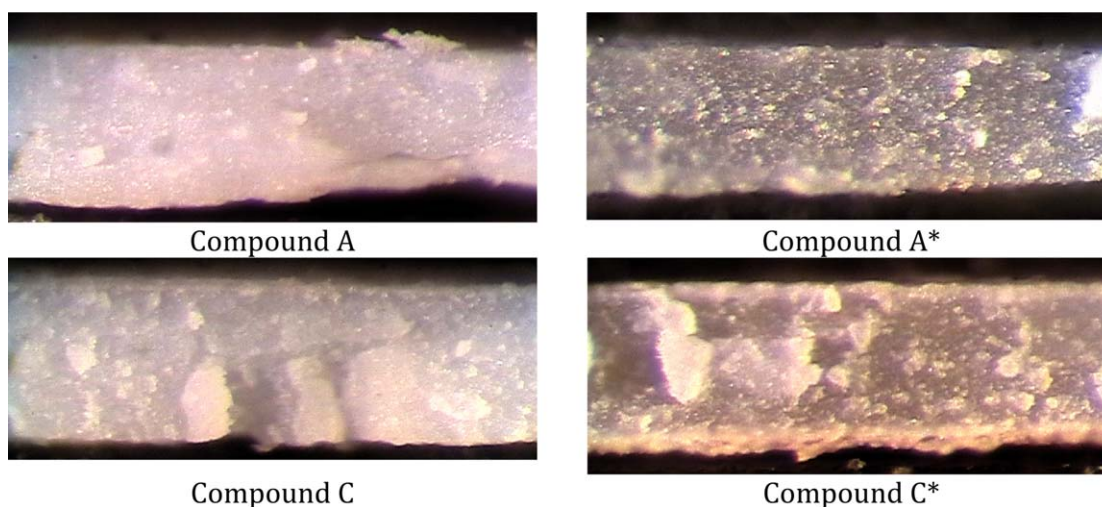


**Figure 11.** Micrographs of sections of the samples after 40 days of composting. The sections refer to the whole thickness of the samples. [Color figure can be viewed in the online issue, which is available at wileyonlinelibrary.com.]

low cost and is effective in increasing the modulus and the HDT of polymers, and TiO<sub>2</sub> which is a commonly adopted white pigment for the industry of plastic cups and plates.

The compounds were obtained by melt compounding in a single screw extruder and their rheological and mechanical properties were carefully assessed. It was found that the Cox-Merz law holds for the pure polymers while it fails in the case of the compounds. Moreover, the processability of the compounds was found to be better than the processability of the Polystyrene commonly adopted for these applications.

The inorganic fillers cause an increase of the modulus of a factor of more than 2 in Compound A with respect to pure PBS. The Compounds B and C, as well B\* and C\* (without the TiO<sub>2</sub> whitening agent) present a larger modulus, intermediate between those of pure PLA and PBS. The value of the modulus makes these compounds interesting for the production of disposable plates and cups, also considering that the elongation at break is significant.

In terms of thermal resistance, the compound A presents a heat distortion temperature a few degrees higher than that of pure PBS, due to the addition of the inorganic fillers. The Compounds B\* and C\*, that include the PLA, present a HDT similar to that of pure PBS and much higher with respect to that of the pure PLA. Both Compounds have, therefore, HDTs high enough to contain hot food or beverages. Finally, the results of biodegradation tests in composting conditions show that the presence of TiO<sub>2</sub> induces a lag time and lower values of biodegradation. Moreover, the compound C\*, containing PLA, presents a faster and larger biodegradation. The polymeric compounds B\* and C\* can be, then, considered as biodegradable substitutes for polystyrene for the production of disposable plates and cups for hot food and beverages.

## REFERENCES

1. Yoo, E. S.; Im, S. S. *J. Polym. Sci. Part B-Polym. Phys.* **1999**, *37*, 1357.
2. Gan, Z. H.; Abe, H.; Kurokawa, H.; Doi, Y. *Biomacromol.* **2001**, *2*, 605.
3. Xu, J.; Guo, B. H. *Biotechnol. J.* **2010**, *5*, 1149.
4. Uesaka, T.; Nakane, K.; Maeda, S.; Ogihara, T.; Ogata, N. *Polymer* **2000**, *41*, 8449.
5. Elberaichi, A.; David, C. *Eur. Polym. J.* **2001**, *37*, 19.
6. Reddy, M. M.; Mohanty, A. K.; Misra, M. *Macromol. Mater. Eng.* **2012**, *297*, 455.
7. Qiu, Z. B.; Ikehara, T.; Nishi, T. *Polymer* **2003**, *44*, 2799.
8. Mani, R.; Bhattacharya, M. *Eur. Polym. J.* **2001**, *37*, 515.
9. Sawyer, D. *J. Macromol. Symp.* **2003**, *201*, 271.
10. Magon, A.; Pyda, M. *Polymer* **2009**, *50*, 3967.
11. De Santis, F.; Pantani, R.; Titomanlio, G. *Thermochim. Acta* **2011**, *522*, 128.
12. Ramkumar, D. H. S.; Bhattacharya, M. *Polym. Eng. Sci.* **1998**, *38*, 1426.
13. Ikada, Y.; Tsuji, H. *Macromol. Rapid Commun.* **2000**, *21*, 117.
14. d'Ayala, G. G.; Di Pace, E.; Laurienzo, P.; Pantalena, D.; Somma, E.; Nobile, M. R. *Eur. Polym. J.* **2009**, *45*, 3215.
15. Noroozi, N.; Thomson, J. A.; Noroozi, N.; Schafer, L. L.; Hatzikiriakos, S. G. *Rheol. Acta* **2012**, *51*, 179.
16. Tsuji, H.; Suzuyoshi, K. *Polym. Degrad. Stab.* **2002**, *75*, 347.
17. d'Ayala, G. G.; Laurienzo, P.; Malinconico, M.; Nobile, M. R.; Pantalena, D.; Russo, R. *Curr. Org. Chem.* **2012**, *16*, 2708.
18. Park, J. W.; Im, S. S. *J. Appl. Polym. Sci.* **2002**, *86*, 647.
19. Shibata, M.; Inoue, Y.; Miyoshi, M. *Polymer* **2006**, *47*, 3557.
20. Bhatia, A.; Gupta, R. K.; Bhattacharya, S. N.; Choi, H. J. *Korea-Australia Rheol. J.* **2007**, *19*, 125.
21. Yokohara, T.; Yamaguchi, M. *Eur. Polym. J.* **2008**, *44*, 677.
22. Yokohara, T.; Okamoto, K.; Yamaguchi, M. *J. Appl. Polym. Sci.* **2010**, *117*, 2226.
23. Chou, P. M.; Mariatti, M.; Zulkifli, A.; Todo, M. *Polym. Bull.* **2011**, *67*, 815.
24. Benchamas, P.; Hongsriphan, N. *ANTEC 1* **2012**.
25. Kim, H. S.; Yang, H. S.; Kim, H. J. *J. Appl. Polym. Sci.* **2005**, *97*, 1513.
26. Tokoro, R.; Vu, D. M.; Okubo, K.; Tanaka, T.; Fujii, T.; Fujiura, T. *J. Mater. Sci.* **2008**, *43*, 775.
27. Xu, Z. H.; Niu, Y. H.; Yang, L.; Xie, W. Y.; Li, H.; Gan, Z. H.; Wang, Z. G. *Polymer* **2010**, *51*, 730.
28. Bhatia, A.; Gupta, R. K.; Bhattacharya, S. N.; Choi, H. J. *J. Appl. Polym. Sci.* **2009**, *114*, 2837.
29. Di Maio, L.; Scarfato, P.; Milana, M. R.; Feliciani, R.; Denaro, M.; Padula, G.; Incarnato, L. *Pack. Technol. Sci.* **2014**, *27*, 535.
30. Speranza, V.; De Meo, A.; Pantani, R. *Polym. Degrad. Stab.* **2014**, *100*, 37.
31. Pantani, R.; Sorrentino, A. *Polym. Degrad. Stab.* **2013**, *98*, 1089.
32. Ferry, J. D. *Viscoelastic Properties of Polymers*; Wiley: New York, **1980**.
33. Cox, W. P.; Merz, E. H. *J. Polym. Sci.* **1958**, *28*, 619.
34. Nobile, M. R. In *Polymer-Carbon Nanotube Composites*; McNally, T.; Pötschke, P., Eds.; Woodhead Publishing: **2011**.
35. Wang, Y. R.; Xu, J. H.; Bechtel, S. E.; Koelling, K. W. *Rheol. Acta* **2006**, *45*, 919.
36. Ren, J. X.; Krishnamoorti, R. *Macromolecules* **2003**, *36*, 4443.
37. Zhao, J.-H.; Wang, X.-Q.; Zeng, J.; Yang, G.; Shi, F.-H.; Yan, Q. *J. Appl. Polym. Sci.* **2005**, *97*, 2273.
38. Fukuda, N.; Tsuji, H. *J. Appl. Polym. Sci.* **2005**, *96*, 190.